1

Signal Metrics for Vertical Handoff Towards (Cognitive) WiMAX

François-Xavier Socheleau[1], Sébastien Houcke[1], Philippe Ciblat[2] and Abdeldjalil Aïssa-El-Bey[1]
[1]*Institut TELECOM; TELECOM Bretagne; UMR CNRS 3192 Lab-STICC ; Université européenne de Bretagne,*
[2]*Institut TELECOM; TELECOM ParisTech,*

1. Introduction

Mobile WiMAX is currently operating in several frequency bands ranging from 2.3GHz to 5.8GHz. To accommodate the anticipated growth in mobile services, there is ongoing pressure on regulators to make additional spectrum available for mobile applications. For instance, the WiMAX Forum is currently investigating new spectrum opportunities below 1GHz (WiMAX Forum, 2008) that would offer good mobile propagation conditions and larger coverage. As a consequence of the physical limits on the amount of available spectrum, it is very likely that regulatory policies in the some bands will evolve from the current fixed spectrum rules to opportunistic spectrum sharing models (U.S. FCC, 2002; 2008). In these new models, regulators allocate section of spectrum that can be used by several (or any) systems under a minimum set of restrictions called spectrum etiquette. Spectrum sharing will require cognitive radio technology (Akyildiz et al., 2006) with dynamic spectrum access (DSA) capabilities and a high level of flexibility to alter wireless system transmission parameters (i.e. adapt the carrier frequency, modulation parameters, power, etc.) according to the surrounding radio environment and the specified policy. Thanks to its adaptive PHY layer and specially to the OFDMA scalability, WiMAX is very well prepared to meet the spectrum sharing model requirements (Blaschke et al., 2008; Leu et al., 2009).

In parallel to the development of new mobile services, there is an emerging trend to provide users with ubiquitous (anywhere, anytime) seamless wireless access. This can be made possible by taking advantage of the coexistence of complementary heterogeneous networks such as 3G(LTE), WiMAX, Wifi etc. In such environment, a challenge is to develop multi-interface terminals able to smartly switch from one wireless interface to another while maintaining IP connectivity and required QoS. This switching process is known as *vertical handoff*. In contrast with horizontal handoff (handoff within a network made of homogeneous wireless interfaces), vertical handoff triggering is based on a multi-criteria decision involving signal quality, bandwidth, traffic load, price, battery status, latency etc. (McNair & Zhu, 2004).

Based on the current WiMAX PHY layer and especially on OFDM(A) properties, we present original works and synthesise existing methods to estimate signal metrics relevant as inputs for any algorithm that has to decide whether to trigger a vertical handoff from any system to WiMAX. We consider the possibility that the WiMAX interface of interest may be cognitive so that the carrier frequency in use by a base station (BS) may evolve over the time. We assume that the section of spectrum allocated to cognitive operation is channelized so that BSs can only transmit on a finite set of possible carrier frequencies. The signal metrics estimation is sequenced in three steps.

1. WiMAX detection: First, upon start-up, pattern detection has to be performed by the terminal in order to identify the spectrum channels in use by a WiMAX BS. In a cognitive radio context, classical coherent frame or superframe preamble detection may not be relevant as it can be a very slow process if many channels have to be scanned. We present more efficient methods based on OFDM cyclostationarity (Bouzegzi et al., 2008) or WiMAX pilot tones properties (Socheleau et al., 2008a; 2009).
2. SINR estimation: Signal to Interference plus Noise Ratio is known to be a good indicator for communication link quality estimation. In the book chapter we discuss the relevance of data-aided SINR estimators for cognitive WiMAX and detail an innovative blind algorithm exploiting OFDMA cyclostationarity (Socheleau et al., 2008b) and a likelihood metric.
3. OFDMA slot activity rate estimation: the time-frequency activity of WiMAX signals is direclty proportional to the traffic load which represents an informative input to the handoff decision algorithm. We show that this rate can directly be deduced by decoding the downlink and uplink mapping (DL/UL-MAP) messages (Dai et al., 2008) but can also be blindly estimated. The latter method suiting cognitive WiMAX better.

This contribution is organised as follows. Cognitive WiMAX scenarios are discussed in section 2. Section 3 presents the signal model. Channels detection algorithms are then proposed in section 4. SINR and slot activity rate estimators are detailed in sections 5 and 6 respectively. Finally, conclusions are presented in section 7.

2. Cognitive WiMAX scenarios

On-going reforms (U.S. FCC, 2008; Wireless Innovation) to spectrum management now offer the opportunity to better exploit highly underutilised portions of spectrum. Regulatory bodies are indeed considering to extend the range and number of license-exempt bands as well as to authorise secondary usage of some licensed spectrum. These new policies open up the possibility to make a clever use (in term of spectral efficiency) of the radio resources by developping devices embedding cognitive radio (CR) technologies (Haykin, 2005). CR enables dynamic spectrum access (IEEE DySPAN) by sensing the electro-magnetic environment and specifically by detecting and then operating on idle frequency channels (or white spaces) at a particular time and place (Haykin, 2005).

From a service provider perspective, CR directly translates in spectral efficiency improvement (Haddad et al., 2007) and therefore in capacity increase. WiMAX could benefit from the CR technology in 3 main scenarios:

1. Today, WiMAX systems mainly operate as primary users in licensed bands (i.e. WiMAX service providers own and control their spectrum). In that context, the network operations could be simplified and the capacity increased by implementing what is called the *cognitive channel assignment* in (Leu et al., 2009). The idea is that frequency channels are not statically assigned to cells but BS are instead equipped with sensitive detectors and dynamically

assign channels to subscriber stations (SSs) based on spectrum availability. Power control is also employed to increase frequency reuse in conjunction with spectrum sensing.

2. In a near future, WiMAX providers may have an economical interest in operating in license-exempt bands (no license fee, economies of scale due to WiMAX devices profusion etc.). This is even more likely if the regulatory bodies open up more of these bands and if they are below 1GHz (which would increase the coverage and thus reduce the number of BS). In this scenario and still for capacity reasons, WiMAX will gain from CR technology as it will have to compete with other systems to get access to the spectrum.

3. In a longer term, we could also imagine WiMAX networks operating as secondary networks in frequency ranges under licenses owned by other systems. This typical CR scenario has already been suggested in (Blaschke et al., 2008) where WiMAX coexists with GSM.

These scenarios mainly differ in the kind of interference they have to deal with (self-interference or other system interference) and in the level of possible cooperation between the various systems sharing the same spectrum (cooperation is hardly possible in the last two scenarios).

Even if a few PHY or MAC layer modifications (sensing signalling (Blaschke et al., 2008), superframe encapsulation (Stevenson et al., 2009) etc.) may be needed for mobile WiMAX to operate in a cognitive context, it is globally well prepared to meet the CR requirements. It is indeed scalable by turning on or off some OFDMA subcarriers to fit into the white spaces, its supports adaptive modulation and coding as well as power control and it can perform spectrum sensing in the frequency domain thanks to its built-in FFT.

3. Signal model

Assuming that in a given frequency channel, a transmitted OFDMA symbol consists of N subcarriers, the discrete-time baseband equivalent transmitted signal is given by [1]

$$x(m) = \sqrt{\frac{E_s}{N}} \sum_{k \in \mathbb{Z}} \sum_{n=0}^{N-1} \varepsilon_k(n) c_k(n) e^{2i\pi \frac{n}{N}(m-D-k(N+D))} g(m-k(N+D)), \tag{1}$$

where E_s is the signal power; $c_k(n)$ are the transmitted symbols at the n -th subcarrier of the k -th OFDM block. These data symbols are assumed to be independent and identically distributed (i.i.d), D is the CP length; $m \mapsto g(m)$ is the pulse shaping filter. $\varepsilon_k(n)$ represents a i.i.d sequence of random variables valued in $\{0,1\}$ that express the absence or presence of signal activity in a time-frequency slot (k,n) .

Let $\{h(l)\}_{l=0,\cdots,L}$ be the baseband equivalent discrete-time propagation channel impulse response of length $L+1$. We assume that D is chosen such that $D > L+1$. The received samples of the OFDMA signal are then expressed as

$$y(m) = e^{-i(2\pi\delta_f \frac{m-\tau}{N} + \theta)} \sum_{l=0}^{L-1} h(l) x(m-l-\tau) + \eta(m) + \gamma(m), \tag{2}$$

[1]Note that for signal metric estimation presented in this chapter there is no need to differentiate the OFDMA users.

where δ_f is the carrier frequency offset (normalised by the subcarrier spacing), θ the initial arbitrary carrier phase, τ the timing offset and η a zero mean circularly-symmetric complex-valued white Gaussian noise of variance σ_η^2 per complex dimension. γ denotes a possible interference with other systems.
At reception, the signal-plus-interference-to-noise ratio (SINR) is expressed as

$$SINR = \frac{S}{\sigma^2} \tag{3}$$

where

$$S = E_s \mathbf{E}[|\,\varepsilon_k(n)c_k(n)\,|^2]\sum_{l=0}^{L}|\,h(l)\,|^2 \tag{4}$$

and

$$\sigma^2 = \sigma_\eta^2 + \mathbf{E}[|\,\gamma(m)\,|^2]. \tag{5}$$

$\mathbf{E}[.]$ stands for the expectation operator.

4. Active channel detection

Since cognitive networks dynamically modify their operating frequency so as to transmit on unused channels, network entry for SSs may not be straightforward as upon star-up SSs are not necessarily aware of the channel(s) currently used by a BS. As an example, the TV band recently released by the FCC for unlicensed operation based on CRs can range up to several hundreds of megahertz which leads to several ten or so possible channels. Figure 1 shows a basic illustration of spectrum usage resulting from dynamic spectrum access where three systems share the same frequency range divided into 5 channels.

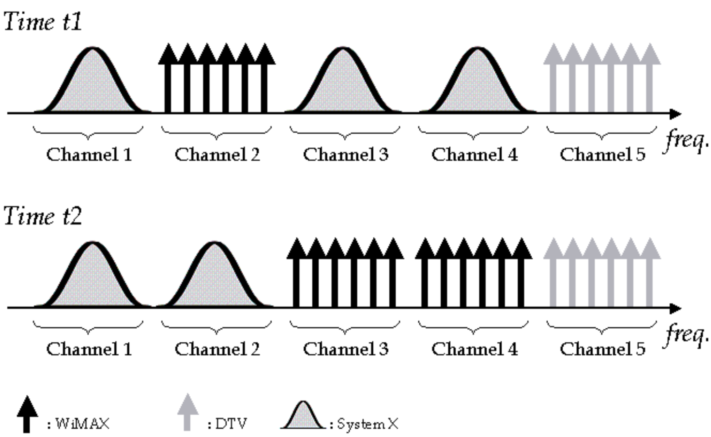

Fig. 1. Example of a channel occupation scenario at different time intervals.

Therefore, any multi-interface terminal with vertical handoff capability, sensing for a cognitive WiMAX BS, has first to detect the frequency channel(s) where the BS operates. In this section, we develop 3 different approaches to perform this detection

• Coherent detection: based on the knowledge of downlink training sequences or preamble, the terminal can reliably detect a BS by a simple cross-correlation. This method offers the best performance but can be time consuming.

• OFDM cyclostationary feature detection: as we will show, WiMAX signals are cyclostationary which can represent a signature useful for detection. Cyclostationarity is relatively easy to detect, not time consuming but has the main drawback of not differentiating downlink (DL) from uplink (UL) frames which may be a concern in FDD networks.

• OFDM pilot structure detection: Pilot tones are of great interest for detection since they are (almost) always present in the transmitted signals and therefore easy to intercept and can be used to discriminate DL from UL frames.

4.1 Coherent detection

To facilitate initial synchronisation, each WiMAX DL frame starts with a preamble (IEEE Std. 802.16, 2005) belonging to a finite set of sequences known a priori by SSs. In a cognitive context where the number and the frequency of the channels used for DL frame transmission are not known by SSs and where active channels are not necessarily contiguous, the current WiMAX preamble may not be relevant to enable initial synchronisation. It may be required to add a bit of signalling overhead. As a reference, for initial synchronisation, the IEEE 802.22 (Stevenson et al., 2009) has defined a superframe structure that encapsulates classical frames and that starts with a preamble duplicated on every channel used by a BS. When a terminal finds a superframe header on a particular channel it then obtains all the necessary information (number and frequency of all the channels used by the BS etc.) to demodulate the frames that follow. This mechanism is pretty efficient as channel detection can be performed by simple cross-correlation between the received signal and the known preamble sequence. In addition, a SS needs just to detect a single channel to get all the information to get connected to the network. However, the drawback of the superframe is that it decreases the network capacity so that to limit the overhead, the superframe header must not be sent frequently. As an example, the 802.22 superframe header is broadcasted every 160 ms which corresponds to 16 frames. In our context where a multi-interface terminal is sensing all the surrounding networks to decide which one is the most appropriate to get connected to, long delays in getting superframe synchronised with each network before deciding which one is the most suited to its needs may not be tolerated. This is even more critical if the set of possible active channels is large. To avoid time consuming process, two detection methods based on the WiMAX signal properties as opposed to frame structure are presented in the sequel.

4.2. OFDM cyclostationary feature detection

To limit the impact of the propagation channel time spread, a cyclic prefix (CP) is added before each WiMAX OFDM symbol (IEEE Std. 802.16, 2005). This CP induces periodic correlation on the OFDMA signals that can be used as a detection pattern (Bouzegzi et al., 2008 ; Ki et al., 2006 ; Ishii & Wornell, 2005 ; Yucek & Arslan, 2007 ; Oner & Jondral, 2007).

More precisely, the WiMAX signal is said to be cyclostationary. Using cyclostationarity for detection is appealing in contrast to energy detection since the noise is hardly never cyclostationary. WiMAX detection can thus be based on the cyclic autocorrelation defined as (Gardner et al. , 2006)

$$R_x^\alpha(u) = \lim_{M\to+\infty} \frac{1}{M}\sum_{m=0}^{M-1}\mathbf{E}\left[x(m)x^*(m+u)\right]e^{-2i\pi m\alpha} \tag{6}$$

where α represents the cycle frequencies. From Eq. (1), the cyclic autocorrelation of an OFDMA signal verifies

$$\begin{aligned} R_x^\alpha(N) &= \lim_{M\to+\infty}\sum_{m=0}^{M-1}\sum_{k\in\mathbb{Z}} g(m-k(N+D)+N)g(m-k(N+D))e^{-2i\pi m\alpha}E_s\frac{\mathbf{E}\left[|\varepsilon_k(n)c_k(n)|^2\right]}{NM}\sum_{n=0}^{N-1}e^{2i\pi n} \\ &= E_s\mathbf{E}\left[|\varepsilon_k(n)c_k(n)|^2\right]\frac{\sin(\pi\alpha D)}{(N+D)\sin(\pi\alpha)}e^{-i\pi\alpha(D-1)}\sum_{q\in\mathbb{Z}}\delta\left(\alpha-\frac{q}{N+D}\right) \end{aligned} \tag{7}$$

where $\delta(.)$ is the Kronecker symbol. The WiMAX signature then corresponds to the set of powerful cycle frequencies. Figure 2 illustrates the the correlation properties induced by the OFDM CP.

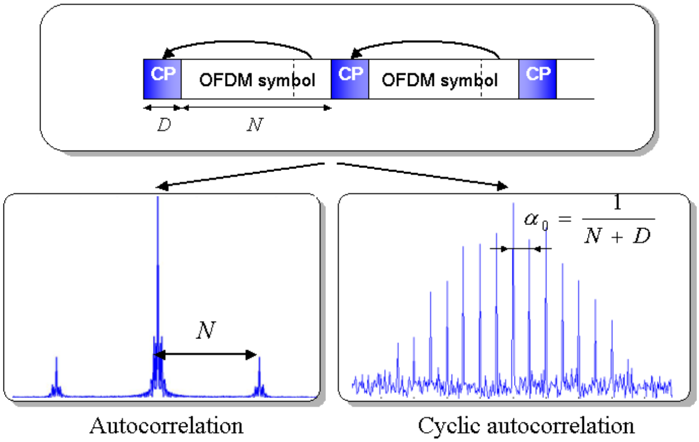

Fig. 2. Illustration of the correlation properties induced by the OFDM cyclic prefix.

As shown in (Jallon, 2008), the cyclic autocorrelation at reception writes

$$R_y^\alpha(N) = R_x^\alpha(N)\sum_{l=0}^{L-1}|h(l)|^2\, e^{-2i\pi\frac{\alpha l}{N+D}}. \tag{8}$$

Detection can then be done by estimating the energy of the cycle frequencies $\alpha_q = \dfrac{q}{N+D}$ thanks to the following cyclic autocorrelation estimator

$$\hat{R}_y^{\alpha_q}(N) = \frac{\sum_{m=0}^{M(N+D)-1} y(m)y^*(m+N)e^{-2i\pi m\alpha_q}}{M(N+D)} \tag{9}$$

where $M(N+D)$ is the length of the observation window. We assume that N and D are known by the multi-interface terminal. The choice of N results from the channel bandwidth defined by regulatory bodies and D is standardised and does not change on the flight. Several structures of detectors have been proposed in the literature, refer to (Bouzegzi et al., 2008; Jallon, 2008; Oner, 2007) for instance.

As illustrated in subsection 4.4, cyclostationary feature detection shows excellent performance even for short CP. However, since the WiMAX DL and UL signals have the same cylostationary signature they cannot be distinguished. This can be a concern for the WiMAX FDD as the signal metrics used to status on a possible vertical handoff have to be estimated on DL subframes. Moreover, in a CR scenario, it is very likely that OFDM systems competing for the access to the same frequency band will have very close (or even the same) modulation parameters (subcarrier spacing, CP length etc.) and thus similar cylostationary signatures. The PHY layer design is indeed strongly driven by features related to the spectrum in which a system operate (propagation channel, available bandwidth etc.). Therefore, methods that involve more particular signatures to detect WiMAX BS may be required and very useful.

4.3. OFDMA pilots structure detection

Pilot tones are of great interest for WiMAX BS detection since (i) they enable to discriminate DL from UL frames as well as systems with similar modulation parameters (ii) they are always present in the transmitted signals and therefore easy to intercept (iii) they are power boosted. If we now consider the pilot tones, the signal model of Eq. (1) becomes

$$x(m) = \sqrt{\frac{E_s}{N}}[x_d(m) + x_t(m)], \tag{10}$$

where

$$x_d(m) = \sum_{k\in\mathbb{Z}} \sum_{\substack{n=0 \\ n\notin \mathrm{I}(k)}}^{N-1} \varepsilon_k(n) a_k(n) e^{2i\pi\frac{n}{N}(m-D-k(N+D))} g(m-k(N+D)), \tag{11}$$

and

$$x_t(m) = \sum_{k\in\mathbb{Z}} \sum_{n\in \mathrm{I}(k)} b_k(n) e^{2i\pi\frac{n}{N}(m-D-k(N+D))} g(m-k(N+D)). \tag{12}$$

$\mathrm{I}(k)$ denotes the set of pilot subcarrier indexes of the k -th symbol, $a_k(n)$ and $b_k(n)$ are the data and pilot symbols respectively. Note that

$$c_k(n) = \begin{cases} b_k(n), & \textit{if } n \in \mathrm{I}(k) \\ a_k(n) & \textit{otherwise.} \end{cases} \tag{13}$$

OFDMA pilot symbols, used for channel estimation and/or synchronisation purposes, are often replicated according to a pre-defined time/frequency distribution. This property induces correlation between pilot subcarriers that can be exploited in conjunction with the periodicity of the time/frequency pilot mapping to perform WiMAX BS detection. The IEEE 802.16 standard defines several pilot tones structures that depend on the PHY layer (OFDM or OFDMA), the DL and UL frames and on the subcarrier permutation mode. For the OFDMA PHY layer (Mobile WiMAX), $b_k(n) = 8/3(1/2 - w_k)$ where w_k is a pseudo-random binary sequence and the pilot mapping is periodic such that $\mathrm{I}(k+K) = \mathrm{I}(k)$, $K \in \mathbb{Z}$ and depends on the permutation mode ($K = 2$ in DL-PUSC and DL-FUSC and $K = 9$ in optional FUSC etc.). Such a periodicity is a useful property that induces cyclostationarity in OFDMA frames. In fact, as shown in (Socheleau et al., 2009), if the pilot tones are designed such that

$$b_k(p) = b_{k+d^{(p,q)}}(q)e^{i\phi}$$

with $d^{(p,q)} \in \mathbb{Z}$ and $\phi \in [-\pi;\pi[$, then the processes $\{c_k(p)\}_k$ and $\{c_k(q)\}_k$ are jointly cyclostationary with the set of powerful cycle frequencies given by $\mathrm{A}_{c_k(p)c_k(q)} = \left\{ \frac{m - \lfloor K/2 \rfloor}{K}, m \in \{0,1,\cdots,K-1\} \right\}$ where $\lfloor\ \rfloor$ stands for integer flooring. The WiMAX signature S then corresponds to the combination of $p, q, d^{(p,q)}$ and K. It is defined as

$$S \stackrel{\Delta}{=} \left\{ \left(p,q,d^{(p,q)},K\right) \mid \mathrm{A}_{(p,q)} \neq \varnothing \right\}. \tag{14}$$

For the DL-PUSC mode (the only mandatory permutation mode), $K = 2$, $d^{(p,q)} = 0$ or 1 and the set of (p,q) is defined by all the possible combinations within $\bigcup_{k\in\mathbb{Z}} \mathrm{I}(k)$. The figure below shows the subcarrier allocation in a DL-PUSC cluster.

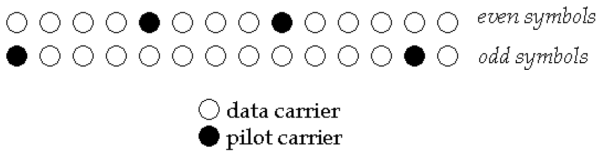

Fig. 3. DL-PUSC subcarrier allocation.

The detection can then be performed thanks to the cyclic cross-correlation energy estimation

$$J \stackrel{\Delta}{=} \sum_{(p,q)\in\xi} \left(\sum_{\alpha\in\mathrm{A}_{(p,q)}} \left| \hat{R}^{\alpha}_{Y(p,q)}\left(d^{(p,q)}\right) \right|^2 \right) \tag{15}$$

where

$$\hat{R}^{\alpha}_{Y(p,q)}\left(d^{(p,q)}\right) = \frac{1}{M-d^{(p,q)}} \cdot \sum_{k=0}^{M-d^{(p,q)}-1} Y_k(p) Y^*_{k+d^{(p,q)}}(q) e^{-i2\pi\alpha k} \tag{16}$$

and $\xi = \{(p,q) \mid \mathrm{A}_{(p,q)} \neq \varnothing$ and $d^{(p,q)} + K \leq M\}$. $Y_k(n)$ are the observations expressed as

$$Y_k(n) \stackrel{\Delta}{=} \frac{1}{\sqrt{N}} \sum_{m=0}^{N-1} y[k(N+D)+D+m] e^{-2i\pi\frac{nm}{N}}. \tag{17}$$

A constant false alarm rate (CFAR) detector is suggested in (Socheleau et al. , 2009) where the detection threshold is given by a Laguerre expansion. As shown in Figure 4, the estimation of the cycle frequencies power deteriorates with timing missynchronization and/or frequency offset as inter-symbol (ISI) and inter-carrier (ICI) interferences occur. However, J is maximum in the case of perfect synchronisation so that ε and τ can be estimated as

$$[\hat{\varepsilon}, \hat{\tau}] = \underset{(\varepsilon,t)}{\mathrm{argmax}} J^{(\varepsilon,t)} \tag{18}$$

where $J^{(\varepsilon,t)}$ is defined as in Eq. (15) by replacing $Y_k(n)$ by

$$Y_k^{(\varepsilon,t)}(n) \stackrel{\Delta}{=} \frac{1}{\sqrt{N}} \sum_{m=0}^{N-1} y[k(N+D)+D+m+t] e^{-2i\pi(\frac{nm}{N}-\varepsilon)}. \tag{19}$$

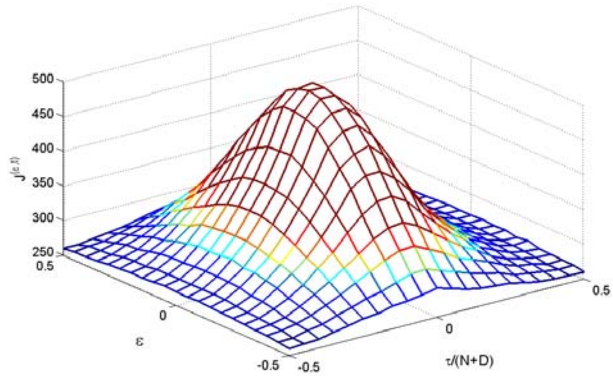

Fig. 4. Effect of synchronisation impairments on the cost function J (SNR=0dB, M=24, $P_{fa} = 0.02$).

Detection is thus based on the knowledge of the pilot structure without the knowledge of pilot symbols so that the detection can be performed on every portion of the received signal. There is no need for frame or superframe synchronisation in contrast with coherent detection methods using known symbol sequences.

Note also that WiMAX pilot subcarriers present other features that can be exploited for detection purposes. An example is given in (Socheleau et al., 2008) where a detector based on the third order statistics of the pseudo-random binary sequence w_k is proposed.

4.4. Detection performance

To illustrate the performance of the detection algorithms, we here consider a Mobile WiMAX BS using 512-subcarriers per channel [2] and a DL-PUSC permutation mode. We recall that there are 60 pilot, 360 data, 91 guard and 1 DC subcarrier [13]. Unless otherwise stated, the cyclic prefix length D is set to 64. The asymptotic false alarm probability P_{fa} is set to 0.02. The Signal-to-Noise Ratio (SNR) is defined as $SNR(dB) = 10log_{10}\left(E_s / \sigma_\eta^2\right)$. The propagation channel is a time-variant discrete-time channel $\{h_k(l)\}_{l=0,\cdots,L}$ with $L = D$ and an exponential decay profile for its non-null component (i.e., $\mathrm{E}[|h_k(l)|^2] = Ge^{-l/\beta}$ for $l = 0,\cdots,L$ and G is chosen such that $\sum_{l=0}^{L}\mathrm{E}[|h_k(l)|^2] = 1$). The channel time variation is simulated using the Jakes model and the maximum Doppler frequency f_d is set to 100Hz. For the simulations, uniformly distributed random ε and τ were generated with $-0.5 \le \varepsilon \le 0.5$ and $-0.5(N+D) \le \tau \le 0.5(N+D)$.

Figure 5 shows the performance of a CFAR detector (see [10]) based on the cyclostationarity induced by the CP. Two observation windows as well as two CP lengths have been tested. The results indicate that only 24 OFDM symbols, which corresponds to half of a 5ms frame, are required to obtain excellent performance and this, even for very short CP (i.e. $N/D = 32$). In contrast with licensed user detection [30], the common framework in cognitive radio, WiMAX detection at negative SNR is not required here. Detectors must only guarantee good performance in SNR ranges where systems experience bit error rates low enough to operate. In our context, detection as such is not much of interest if the communication cannot be established afterwards.

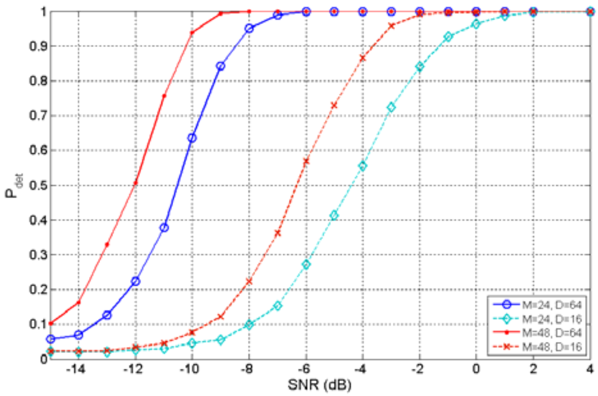

Fig. 5. Detection performance based on the cyclostationary feature induced by the CP ($\beta = 0.25D$).

[2]Note that it would nicely fit into a 6MHz TV channel [6]

The performance of the pilots structure detector is displayed on Figure 6. Similarly to the previous criterion, the detection rate is significantly improved as the number of available symbols increases and is still excellent for a short observation window.

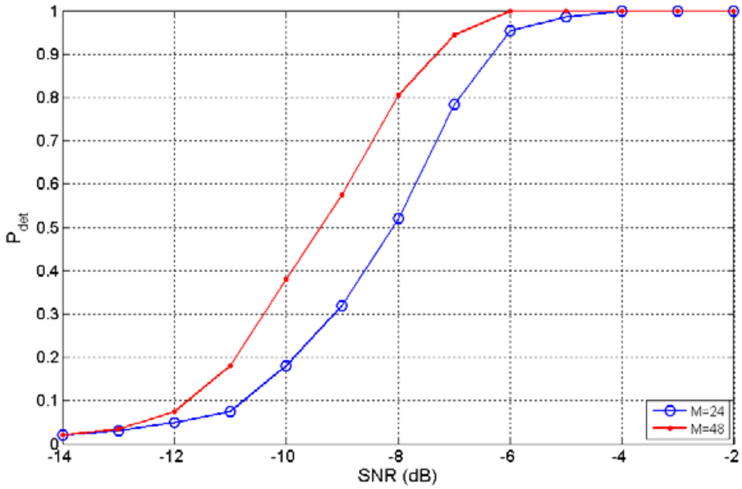

Fig. 6. Detection performance based on the pilot tones structure ($\beta = 0.25D$).

5. SINR estimation

Upon detection of a wireless interface which it is compatible with, our terminal has then to estimate the link quality it can hope with this interface in order to decide if it meets its data rate and robustness requirements. SINR is a relevant indicator commonly used to evaluate this link quality. For the WiMAX interface, SINR is usually measured on preambles or specific broadcast DL zones (see Eq.(144) in (IEEE Std. 8022.16, 2005)). This kind of estimation method, based on the knowledge of pilot symbols, gives excellent performance since it is data-aided. However, for the same reasons as those discussed in subsection 4.1, this method can be time consuming as it requires to get (super)frame synchronised. An alternative approach, based on the correlation and the cyclostationarity induced by the OFDM CP, is presented in this section. This algorithm estimates the signal and the noise plus interference power independently and does not require the knowledge of pilots symbols so that it can be applied on any portion of WiMAX signals.

5.1. Noise plus interference power estimation

As in (Socheleau et al., 2008b), we here suggest to take advantage of OFDM signals particular structure to estimate the noise variance. More precisely, we show hereafter that the noise variance can be estimated thanks to the redundancy induced by the CP. In fact, the CP use leads to $x\left(k\left(N+D\right)+m\right)=x\left(k\left(N+D\right)+N+m\right)$, for any integer k and any $m \in \{0,\cdots,D-1\}$. It is then straightforward to see that if we assume perfect synchronisation at reception (i.e $\tau = 0$ and $\delta_f = 0$) and a time-invariant channel over an OFDM symbol duration, we can get $D-L$ noise plus interference power estimates defined as

$$\hat{\sigma}_u^2 = J(u),\ L \le u \le D-1 \tag{20}$$

with

$$J(u) = \frac{1}{2M(D-u)} \sum_{k=0}^{M-1} \sum_{m=u}^{D-1} \left| y\big(k(N+D)+m\big) - y\big(k(N+D)+N+m\big) \right|^2 \tag{21}$$

where M denotes the number of OFDM symbols in the observation window. Note that non data-aided synchronisation can be done thanks to the detection algorithm of subsection 4.3 or to more general algorithms such as those discussed in (van de Beek et al., 1997; Park et al., 2001 ; Xiaoli et al., 2001).

It can be easily shown that the estimator with the smallest variance is found for $u = L$. The difficulty is then to estimate L. Cui et al. suggested an estimator in (Cui & Tellambura, 2006) but it has the major disadvantage of being based on a threshold level chosen arbitrarily. To overcome this limitation we hereafter propose a method inspired by maximum likelihood estimation.

From Eq. (21), $J(u)$ can be expressed as

$$J(u) = \left(1 - \frac{1}{D-u}\right) J(u+1) + \xi(u) \tag{22}$$

where $\xi(u)$ is a random variable given by

$$\xi(u) = \frac{1}{2M(D-u)} \sum_{k=0}^{M-1} \left| y\big(k(N+D)+u\big) - y\big(k(N+D)+N+u\big) \right|^2 . \tag{23}$$

For $L \le u \le D-1$ and M large enough, $\xi(u)$ is Gaussian and verifies

$$\xi(u) \sim \mathcal{N}\left(\frac{\sigma^2}{D-u}, \frac{\sigma^4}{M(D-u)^2} \right). \tag{24}$$

L is then estimated using the likelihood function $f\left(X_u \mid L = u\right)$ with X_u the multivariate observation variables defined as $X_u = \left(\xi(u), \xi(u+1), \cdots, \xi(D-1)\right)$. The different $\xi(u)$ being independent, $\hat{L}$ is given by

$$\hat{L} = \underset{0 \le u \le D-1}{\operatorname{argmax}} \left[\prod_{m=u}^{D-1} f\left(\xi(m) \mid L = u\right) \right]^{1/(D-u)}, \tag{25}$$

where $f\left(\xi(m) \mid L = u\right)$ is computed thanks to Eq. (24) by making the approximation that $\sigma^2 = J(u)$. Note that because the observations X_u are of variable lengths, Eq. (25) is defined as an average likelihood which is the geometric mean of the individual likelihood elements.

5.2. Signal power estimation

Thanks to equations (7) and (9) it is straightforward to show that the signal power can be estimated as

$$\hat{S} = \frac{1}{2N_c+1}\left|\sum_{q=-N_c}^{N_c} \hat{R}_y^{q\alpha_0}(N)\frac{\sin(\pi q\alpha_0)}{\alpha_0\sin(\pi q\alpha_0 D)}e^{i\pi q\alpha_0(D-1)}\right| \quad (26)$$

where $\alpha_0 = 1/(N+D)$ and N_c represents the number of considered cycle frequencies to estimate the signal power. We assume that the interference does not show the same cyclostationary properties as WiMAX. The choice of N_c is a trade-off between the estimator bias and variance. From Eq. (26), it can be shown that the estimator asymptotic variance (i.e. for $M \to +\infty$) decreases as the number of cycle frequencies increases. However, Eq. (7) indicates that it may be judicious to choose cycle frequencies within the first lob of $\hat{R}_y^{q\alpha_0}(N)$ as for $q \geq N/D$, the power of this function is very small. In addition, to limit the estimator bias, N_c has to be bounded by the channel coherence bandwidth. In fact, from Eq. (8) and thanks to Parseval's identity, $R_y^{q\alpha_0}(N)$ can be expressed as

$$R_y^{q\alpha_0}(N) = R_x^{q\alpha_0}(N)\int_{-\frac{1}{2}}^{\frac{1}{2}}\mathbf{E}\left[H(\nu)H^*(\nu-q\alpha_0)\right]d\nu \quad (27)$$

where $H(\nu) = \sum_{l=0}^{L} h(l)e^{-2i\pi l\nu}$. Thus, from the definition of S (see Eq. (4)), the cycle frequencies used to estimate the signal power have to be limited to the case where $R_y^{q\alpha_0}(N) = R_x^{q\alpha_0}(N)\sum_{l=0}^{L}|h(l)|^2$ which is equivalent to choose $q\alpha_0$ within the coherence bandwidth where $\mathbf{E}\left[H(\nu)H^*(\nu-q\alpha_0)\right] \simeq \mathbf{E}\left[|H(\nu)|^2\right]$. The coherence bandwidth B_c is usually defined thanks to the channel root mean square delay spread [25]. In our case, as the channel impulse response is unknown at reception, B_c is approximated as $\hat{B}_c = 1/(\rho\hat{L})$ where ρ is a coefficient expressing the desired correlation rate within B_c. Consequently, we choose $N_c = \min\left(\frac{N+D}{\rho\hat{L}}, \frac{N}{2D}\right)$. As shown in (Socheleau et al., 2008b), ρ's choice has only a very little influence on the estimator performance.

5.3 SINR estimation performance

Using the same simulation context as in subsection 4.4, we plot on Figure 7 the Normalised Mean Square Error (NMSE) of the SINR estimation versus the true SINR for different M. $\mathrm{NMSE} = \mathbf{E}\left[\left(\hat{S}/\hat{\sigma}^2 - S/\sigma^2\right)^2\frac{\sigma^4}{S^2}\right]$, $D = 64$, $\beta = 16$ and ρ is set to 5. As expected, the performance is significantly improved as the number of available OFDM symbols increases

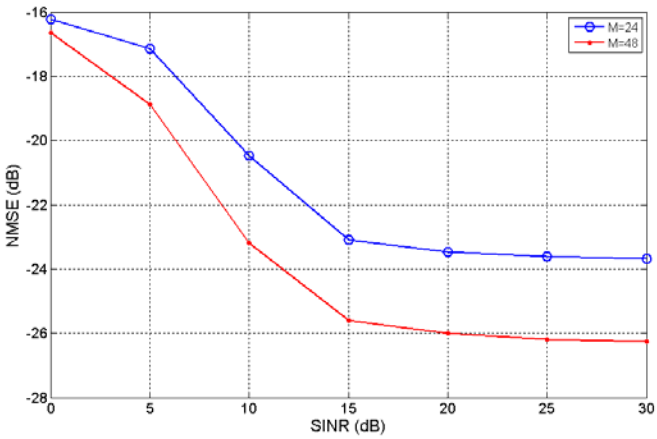

Fig. 7. NMSE of the SINR estimator.

As detailed in (Dai et al., 2008), the measured SINR of a WiMAX DL signal can be transformed into a data rate. WiMAX supports a large number of modulation and forward error correction coding schemes and allows the scheme to be changed based on the channel conditions. This is what is called adaptive modulation and coding (AMC). The objective of AMC is to maximise throughput in a time-varying channel. Since the adaptation algorithm typically calls for the use of the highest modulation and coding scheme that can be supported for the current SINR, it is possible to know the used data rate. For WiMAX, there is a modulation and coding scheme defined per SINR fluctuation of 2dB. Consequently, in Figure 8 we plot the probability of estimating the SINR within the range of +/-1 dB of the true value. It clearly indicates that our SINR estimator gives a reliable measure that can be used for vertical handoff decision. Note that this probability becomes greater than 97% for $M = 24$ and a SINR ≥ 0 dB if the tolerated range is increased to +/-1.5 dB.

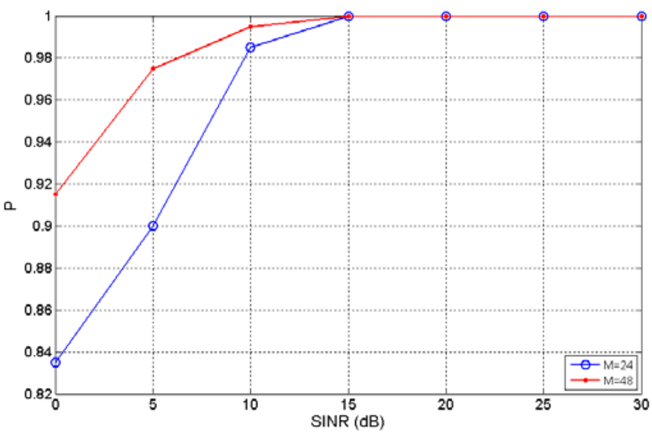

Fig. 8. Probability of estimating the SINR within +/-1 dB of the true value.

6. Slot activity rate estimation

In the context of signal metrics estimation for vertical handoff, the SINR knowledge of OFDMA signals is not fully informative without the knowledge of the time-frequency slots activity rate (SAR). This rate is defined as the probability $\mathrm{P}(\{\varepsilon_k(n)=1\})$ where $\varepsilon_k(n)$ is defined in Eq. (1). There can be scenarios (low network load, segmentation etc.) where a few slots are active within an OFDMA frame. In this case, even if each active slot is very powerful (which indicates a good quality of communication link), the SINR as defined in Eq. (3) and estimated in section 5 can be low. This finds an explanation in the SINR computation that is averaged over all (active or not) slots. Moreover, the main question a multi-interface terminal is trying to answer when measuring signal metrics is: what is amount of resources that will be allocated to me if I get connected to the wireless interface I am currently sensing? The SAR can be useful to answer this question since it indicates the part of the network resources that is already occupied by other users. However, for WiMAX networks, SAR has to be carefully interpreted as it is just an indicator of the traffic load and is mainly relevant when this load is low. In fact, when the SAR is low, it indicates that the sensed cell has not reached its maximum of capacity so that resources are available for new connections. But if the SAR is high (equal to 1 for instance), one can wrongly infer that no new connection will be allowed by the network. Since the 802.16 standard does not specify the resources allocation methods, there can be strategies that aim to maximise the use of physical resources whatever the number of open connections. This can lead to situations where even if the current SAR is equal to one, new connections will be allowed and resources dynamically redistributed among the set of users.
In the WiMAX system, the resource allocation is specified in the UL/DL MAP messages broadcasted at the beginning of each frame. These messages gives the number of slots allocated to each user in uplink and downlink respectively. By decoding the UL/DL MAP the SAR can be directly deduced. This operation, requiring frame synchronisation, can be once again time consuming for a multi-interface terminal. In addition, it is also power consuming since demodulation and decoding are required. In this section, an alternative approach is derived based on the estimation of all $\varepsilon_k(n)$ on the observation window.

6.1. Algorithm

SAR estimation is equivalent to differentiate active slots from inactive slots. Intuitively, by considering that noise plus interference power σ^2 is known, common detector structures can be used. For instance,

$$\widehat{\mathrm{P}}(\{\varepsilon_k(n)=1\}) = \frac{\sum_{k,n} I\left(|Y_k(n)|^2 > g(\sigma^2)\right)}{MN} \tag{28}$$

where $I(A)$ denotes the indicator function of a given event A, $g(\sigma^2)$ is a thresholding function like $g(\sigma^2)=\lambda\sigma^2$ for instance and $Y_k(n)$ is defined by Eq. (17). We here assume perfect synchronisation at reception.
The problem of estimators as the one defined in Eq. (28) is that the choice of the detection threshold λ has a strong influence on the performance. To overcome this constraint, we

suggest an alternative method sequenced in two stages:

1. Sorting of the observed symbols $Y_k(n)$ based on a likelihood criterion. From the knowledge of the noise plus interference probability density function (pdf), the idea is to sort the $Y_k(n)$ according to their probability of being made of noise plus interference only.
2. Cost function minimisation. Once the $Y_k(n)$ are sorted, a breakdown point is sought in the ordered set in order to separate symbols of signal plus noise and interference from symbols of noise plus interference only.

Let Ω be the set of observed symbols defined as

$$\Omega = \bigcup_{k,n} Y_k(n),\ k \in \{0,1,\cdots,M-1\} \text{ and } n \in \{0,1,\cdots,N-1\}. \tag{29}$$

We define the relation of order $\mathbf{R}$ as

$$(x,y) \in \Omega^2 \mid f(x) \le f(y) \tag{30}$$

where $f(x)$ is the pdf of the noise plus interference. For the sake of simplicity, we assume that this pdf is Gaussian so that

$$f(x) = \frac{1}{\pi\sigma^2} e^{-|x|^2/\sigma^2}. \tag{31}$$

Note that this may not always be true, especially in the case of strong non Gaussian interference. In this particular case, $f(x)$ can be estimated thanks to the samples used to compute σ^2 in subsection 5.1.

$(\Omega,\mathbf{R})$ is then the ordered set of the $Y_k(n)$ sorted out by their crescent probability of being symbols of noise plus interference only. $(\Omega,\mathbf{R})$ is equivalent to sort out the $Y_k(n)$ by their decreasing energy. The elements that composed this set are written as

$$(\Omega,\mathbf{R}) = \{\overline{Y}_0, \overline{Y}_1, \cdots, \overline{Y}_{MN-1}\}. \tag{32}$$

Once the symbols are ordered, we suggest to work on the subset $(\Omega_u,\mathbf{R}) = \{\overline{Y}_u, \overline{Y}_{u+1}, \cdots, \overline{Y}_{MN-1}\}$ and to detect the first u for which $(\Omega_u,\mathbf{R})$ is made of noise plus interference only. The approach consists for each $u \in \{0,1,\cdots,MN-1\}$, to estimate a parameter $\hat{\theta}_u$ of the pdf $f(x)$ from the elements of $(\Omega_u,\mathbf{R})$. Once these $\hat{\theta}_u$ are estimated, the breakdown point p_r is expressed as

$$p_r = \arg\min_u (\hat{\theta}_u - \theta)^2. \tag{33}$$

The $\overline{Y}_0, \overline{Y}_1, \cdots, \overline{Y}_{p_r-1}$ are then considered as symbols made of signal plus noise and interference and the $\overline{Y}_{p_r}, \overline{Y}_{p_r+1}, \cdots, \overline{Y}_{MN-1}$ as symbols of noise plus interference only. It now remains to choose the parameter θ as well as the estimation method associated to it. The $Y_k(n)$ being usually centred whatever the value of $\varepsilon_k(n)$, we suggest to choose $\theta = \sigma$. As for the estimation method, it will depend on two criteria:

1. The estimator efficiency. If T is the estimator of σ, is efficiency is defined as

$$e(T) = \frac{1/\Im(\sigma)}{Var[T]} \tag{34}$$

where $\Im(\sigma)$ is the Fisher information. We seek to have the estimator with the highest efficiency. If $(\Omega_u, \mathbf{R})$ is made of noise plus interference only, then the estimation squared error $(\hat{\theta}_u - \theta)^2$ has to be as small as possible.

2. Robustness. Robustness translates the estimator resistance to outliers. It is measured by the proportion of incorrect observations (arbitrarily large) an estimator can accept before returning results that are also arbitrarily large. In contrast to what is usually quested, we here focus on estimators with the lowest possible robustness. If $(\Omega_u, \mathbf{R})$ includes at least a symbol of signal plus noise and interference, ideally we want to have $(\hat{\theta}_u - \theta)^2$ as large as possible.

The maximum likelihood estimator expressed as $\breve{\sigma}_u = \sqrt{\frac{1}{MN-u}\sum_{\ell=u}^{MN-1} |\bar{Y}_\ell|^2}$ is the optimal estimator according to the wanted efficiency and robustness criteria (efficiency=1 and robustness=0). Consequently, the breakdown point is expressed as

$$p_r = \underset{u}{\operatorname{argmin}}\left(\sqrt{\frac{1}{MN-u}\sum_{\ell=u}^{MN-1} |\bar{Y}_\ell|^2} - \sigma\right)^2 \tag{35}$$

and the slot activity rate is given by

$$\widehat{\mathrm{P}}(\{\varepsilon_k(n) = 1\}) = \frac{p_r}{MN}. \tag{36}$$

6.2. Slot activity rate estimation performance

With a simulation context similar to the one depicted in the previous section, Figure 9 shows the NMSE of the SAR estimator for several SNR. To find the breakdown point of Eq. (35), we used either the perfect knowledge of σ or its estimate presented in section 5. The results indicates that the proposed method is robust to estimation errors of σ and not much dependent on the true SAR but very sensitive to the SINR.

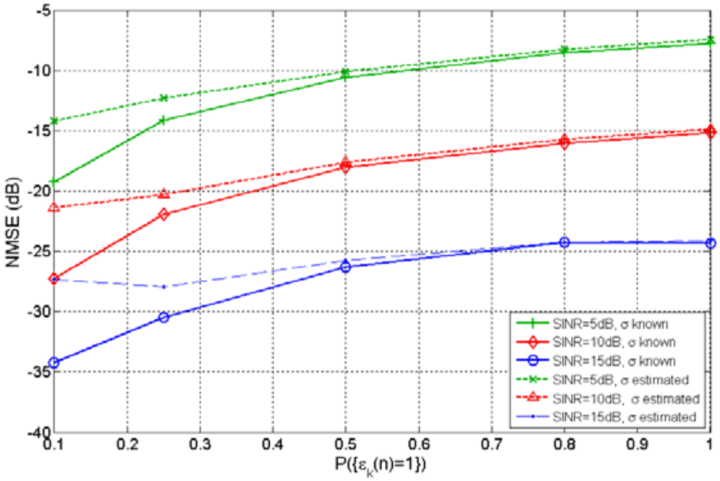

Fig. 9. Normalised mean square error of the slot activity rate estimator for various SNR.

Figure 10 compares the performance of our algorithm with the common constant false alarm rate (CFAR) detection method for a SINR of 10dB. the CFAR detector assume that $\varepsilon_k(n)=1$ when $P_{fa} > e^{-\frac{|Y_k(n)|^2}{\sigma^2}}$. The results highlight the limitations of detectors based on a threshold. It can be observed that the choice of the threshold has a strong influence on the performance in contrast to our method that offers better controlled results.

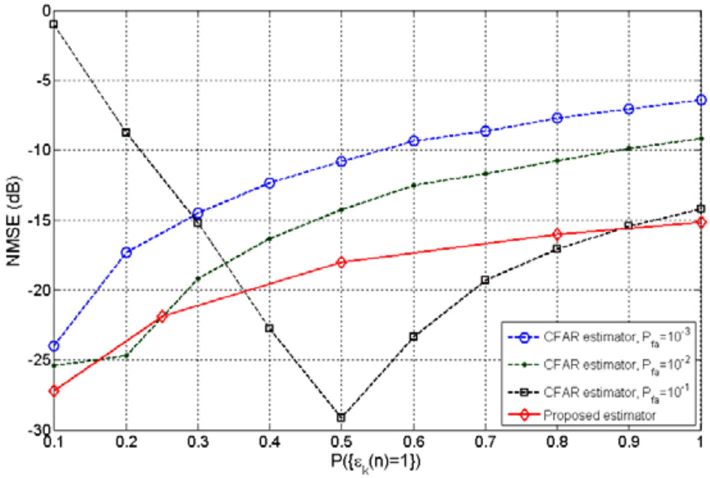

Fig. 10. Comparison of the proposed method with the CFAR detector (SNR=10dB, σ known).

7. Conclusion

The main conclusion of this chapter is that WiMAX signal metrics measurement for vertical handoff decision is possible in a cognitive context without requiring any modifications of the current standard. The data-aided metrics measurement based on preamble detection or frame header decoding have been constrasted to non data-aided approaches that mainly rely on OFDM(A) specific features. We have shown that non data-aided DL subframe detection, SINR estimation and slot activity rate estimation perform well enough to be relevant inputs for algorithms that have to decide whether to trigger a vertical handoff from any system to WiMAX. In addition, the proposed metrics estimators suit well cognitive radio scenarios since they require only small portions of signal and therefore allow a fast decision making process on the WiMAX signal quality and traffic load.

8. References

Akyildiz, I. F. ; Lee, W-Y. ; Vuran, M. C. & Mohanty, S. (2006). NeXt generation/dynamic spectrum access/cognitive radio wireless networks: A survey. *Computer Networks*, pp. 2127-2159.

van de Beek, J. ; Sandell, M. & Borjesson, P.O. (1997). ML estimation of time and frequency offset in OFDM systems. IEEE Trans. on Signal Processing, Vol. 49, pp. 1800-1805.

Blaschke, V. ; Kloeck, C.; Weiss, J.; Renk, T. & Jondral, F.K. (2008). Opportunistic WiMAX-GSM coexistence. Communications, IET, Vol. 2, No. 6.

Bouzegzi, A.; Jallon, P. & Ciblat, P. (2008). A Second Order Statistics Based Algorithm for Blind Recognition of OFDM Based Systems. IEEE Globecom Conf.

Cordeiro, C.; Challapali, K.; Birru, D. & Shankar, S. (2006). IEEE 802.22: An Introduction to the First Wireless Standard based on Cognitive Radios. Journal of Communications, Vol. 1, No. 1, pp. 38-47.

Cui, T. & Tellambura, C. (2006). Power delay profile and noise variance estimation for OFDM. IEEE Communications Letters, Vol. 10 No. 1.

Dai, Z; Fracchia, R.; Gosteau, J.; Pellati, P. & Vivier, G. (2008). Vertical Handover Criteria and Algorithm in IEEE802.11 and 802.16 Hybrid Networks. IEEE Int. Conf. On Communications.

Gardner, W. A. ; Napolitano, A. & Paurac, L. (2006). Cyclostationarity: Half a century of research. Signal processing, Vol. 86, No. 4, pp. 639-697.

Haddad, M.; Hayar, A.M. & Debbah, M. (2007). Spectral Efficiency of Cognitive Radio Systems. IEEE GLOBECOM.

Haykin, S. Cognitive radio: brain-empowered wireless communications (2005). IEEE Journal Sel. Areas in Comm., Vol. 23, No. 2, pp. 201-220.

IEEE Dynamic Spectrum Access Networks Conference (DySPAN). http://www.ieee-dyspan.org/

IEEE Std. 802.16 (2005). Part 16: Air Interface for Fixed and Mobile Broadband Wireless Access Systems, Amendment 2: Physical and Medium Access Control Layers for Combined Fixed and Mobile Operations in License Bands and Corrigendum 1.

Ishii, H. & Wornell (2005), G. W. OFDM blind parameter identification in cognitive radios. IEEE Conf. on Personal, Indoor and Mobile Radio Communications, pp. 700-705.

Jallon, P. (2008). An algorithm for detection of DVB-T signals based on their second order statistics. EURASIP Journal on Wireless Communications and Networking, article ID 538236.
Leu, A.E.; Mark, B.L. & McHenry, M. (2009). A Framework for Cognitive WiMAX with Frequency Agility. Proceedings of IEEE, Special Issue on Cognitive Radio, Vol. 97, No. 4.
Li, H.; Bar-Ness, Y.; Abdi, A.; Somekh, O. & Su, W. (2006). OFDM modulation classification and parameters extraction. IEEE Conf. on Cognitive Radio Oriented Wireless Networks and Communications, pp. 1-6.
McNair, J. & Zhu, F. (2004). Vertical handoffs in fourth-generation multinetwork environments. IEEE Wireless Communications, Vol. 11, No. 3.
Oner, M. & Jondral, F. (2007). On the Extraction of the Channel Allocation Information in Spectrum Pooling Systems. IEEE Journal Sel. Areas in Comm., Vol. 25, No. 3.
Park, B.; Ko, E.; Cheon, H.; Kang, C. & Hong, D. (2001). A blind OFDM synchronization algorithm based on cyclic correlation. IEEE Globecom Conf., pp. 3116-3119.
Rappaport, T.S. (2002). Wireless Communications: Principles and Practices . Prentice Hall.
Socheleau, F.-X.; Houcke, S.; Aïssa-El-Bey, A. & Ciblat, P. (2008a). OFDM system identification based on m-sequence signatures in cognitive radio context. IEEE PIMRC.
Socheleau, F-X; Aïssa-El-Bey, A. & Houcke, S. (2008b). Non Data-Aided SNR Estimation of OFDM Signals. IEEE Communications Letters, Vol. 12, No. 11.
Socheleau, F.-X.; Ciblat, P. & Houcke, S. (2009). OFDM System Identification for Cognitive Radio Based on Pilot Induced Cyclostationarity. IEEE WCNC.
Stevenson, C.; Chouinard, G.; Zhongding L.; Wendong, H.; Shellhammer, S. & Caldwell, W. (2009). IEEE 802.22: The First Cognitive Radio Wireless Regional Area Network Standard. IEEE Communications Magazine, Vol. 47, No. 1.
U.S. FCC (2002). Review of Spectrum Management Practices.
U.S. FCC (2008). Second Report and Order and Memorandum Opinion and Order, in the Matter of Unlicensed Operation in the TV Broadcast Bands Additional Spectrum for Unlicensed Devices Below 900 MHz and in the 3 GHz Band.
WiMAX Forum (2008). Spectrum Opportunities below 1GHz.
Wireless Innovation. http://www.wirelessinnovation.org/
Xiaoli, M.; Giannakis, G.B. & Barbarossa, S. (2001). Non-data-aided frequency-offset and channel estimation in OFDM and related block transmissions. IEEE ICC.
Yucek, T. & Arslan, H. (2007). OFDM Signal Identification and Transmission Parameter Estimation for Cognitive Radio Applications. IEEE Glob. Telecom., pp. 4056-4060.
Zeng, Y.; Liang, Y-C. & Zhang, R. (2008). Blindly Combined Energy Detection for Spectrum Sensing in Cognitive Radio. IEEE Signal Processing Letters, Vol. 15, pp. 649-652.